2020-01-0746 Published 14 Apr 2020



A Virtual Driveline Concept to Maximize Mobility Performance of Autonomous Electric Vehicles

Vladimir Vantsevich University of Alabama at Birmingham

David Gorsich U.S. Army Ground Vehicle Systems Center

Jesse R. Paldan University of Alabama at Birmingham

Michael Letherwood Alion Science & Technology

Citation: Vantsevich, V., Gorsich, D., Paldan, J.R., and Letherwood, M., "A Virtual Driveline Concept to Maximize Mobility Performance of Autonomous Electric Vehicles," SAE Int. J. Advances & Curr. Prac. in Mobility 2(3):1551-1560, 2020, doi:10.4271/2020-01-0746.

This article is from WCX™ 2020 SAE World Congress Experience.

Abstract

n-wheel electric motors open up new prospects to radically enhance the mobility of autonomous electric vehicles with four or more driving wheels. The flexibility and agility of delivering torque individually to each wheel can allow significant mobility improvements, agile maneuvers, maintaining stability, and increased energy efficiency. However, the fact that individual wheels are not connected mechanically by a driveline system does not mean their drives do not impact each other. With individual torques, the wheels will have different longitudinal forces and tire slippages. Thus, the absence of driveline systems physically connecting the wheels requires new approaches to coordinate torque distribution. This paper solves two technical problems. First, a virtual driveline system (VDS) is proposed to emulate a mechanical driveline system virtually connecting the e-motor driveshafts, providing coordinated driving wheel torque management. The VDS simulates power split between driving wheels.

Conceptually, VDS is founded on generalized tire and vehicle parameters. Generalized slippages are utilized to determine virtual gear ratios from a virtual transfer case to each wheel. The virtual gear ratios serve as signals to the electric motors. Secondly, a new velocity-based mobility performance index is used as the ratio of the actual velocity of a vehicle, with individual wheel management, to the theoretical velocity of the same vehicle equipped with a mechanical driveline without controllable gear ratios. Using the index as the objective function, a maximization problem of vehicle mobility is formulated and solved. Optimal virtual gear ratios are determined for maximal mobility in a given terrain condition. Simulations of a 4x4 tactical vehicle in stochastic soil conditions demonstrated a 17% increase in mean values of the velocity-based mobility performance index when the vehicle is electrically driven by the optimal virtual gear ratios as compared to the mechanical driveline system with noncontrolled differentials.

Introduction

obility estimation based on vehicle dynamics modeling sees use in automated control systems that have been designed to reduce mobility problems in poor driving conditions. Today's systems possess a control response time within 100 to 120 milliseconds and greater, meaning that the actual control of a spinning wheel occurs after the wheel is losing or has lost the grip with terrain and the vehicle can very likely be immobilized [32]. For this reason, it is important to further analyze the vehicle dynamics approach to mobility estimation.

Vehicle dynamics-based mobility criteria are typically derived from wheel or vehicle equations of motion. Soil properties are represented by peak friction coefficients and rolling resistance. The peak friction and rolling resistance coefficients are used for defining relationships among tire forces and ground reaction forces.

Criteria for mobility assessment have been proposed based on comparing the total tire longitudinal forces or torques to the maximum potential or resistance forces [2, 3, 4]. Another criterion describes a conceptual possibility of a vehicle with a given number of drive axles to traverse a terrain with given characteristics [5]. These methods do not differentiate resistance to motion at different wheels of the vehicle and thus cannot be utilized in real-time vehicle motion analysis since they were built on estimating "go through" or "not go through" analysis of vehicle mobility. Furthermore, the criteria do not allow estimating an individual wheel's contribution to vehicle mobility during vehicle movements.

Tire slippage has been an area of interest for decades because of its importance to mobility prediction. Correlations between tire slippage and friction coefficients have also been studied for estimation methods such as the slip-slope method [6]. Traction predictive equations usually relate wheel

torque, tire slip, and tractive forces to tire and ground data; the accuracy of these models can depend on the similarity of the new condition being predicted to that of the tests from which the equations were derived [7, 8, 9, 10, 11, 12]. A common feature of the existing mobility indices is that they cannot account for the influence of the power split between the driving wheels.

The circumferential forces at the driving wheels strongly depend on the characteristics of the driveline system, which determines the power distribution (i.e., the power split) between the wheels [4]. This means that the driving wheels will develop different circumferential forces when different power-dividing units (PDUs) are in use in the driveline while the sum of these forces is still equal to the external resistance to movement. The circumferential forces at the wheels generated by different characteristics of the PDUs influence vehicle properties, including mobility, fuel and energy consumption, and also stability, turnability and handling, i.e., maneuver. Therefore, the same vehicle will demonstrate different levels of mobility and other vehicle properties in the same terrain conditions when the vehicle is equipped with different combinations of PDUs in the driveline system [4].

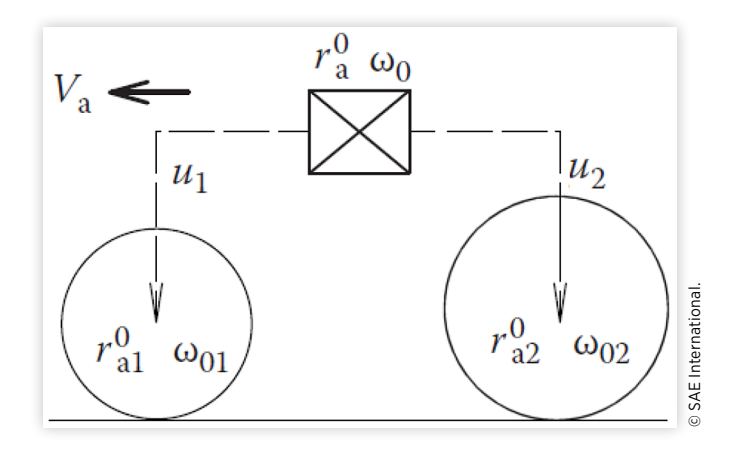
For electric vehicles that use four-wheel-drive with separate motors, torque distribution algorithms have been developed to optimize energy efficiency [13, 14, 15]. Torque distribution methods have also been created to improve lateral stability and turning radius [16, 17]. These studies are for optimization of efficiency and stability of road vehicles, whose controllers respond to changing driver inputs and maneuvers, but where the tire-road friction is assumed constant; they do not take into account the wheel power split on vehicle terrain mobility when the terrain conditions can change quickly and continuously. Optimization of the torque allocation can improve efficiency on rough terrain by reducing the total torque demand [18]. The impact of the wheel power split on the performance of electric vehicles on off-road terrain has been previously studied for the purpose of improving energy efficiency [19, 20]. It is now time to maximize terrain mobility by optimizing wheel power distribution.

The ultimate goal of this paper is to develop an adequate assessment tool to estimate the influence of the power distribution between the driving wheels on vehicle mobility performance. To accomplish this goal, an analysis of the power split between the wheels is discussed first. Generalized parameters are introduced for a conventional mechanical driveline. The generalized tire and vehicle parameters are then applied to a vehicle with four individual electric motors driving the wheels. In this regard, the generalized parameters virtually simulate the interactions of the four wheels and their contribution to the overall vehicle dynamics and mobility.

Kinematic Discrepancy in Multi-Wheel Vehicles

<u>Figure 1</u> illustrates a diagram of a vehicle's driving wheels of different diameters that can be caused by the use of different sized-wheels or by the manufacturing tolerance. In the layout of the drive axles shown in <u>Fig. 1</u>, the left and right wheels of each axle were replaced by a single equivalent wheel with

FIGURE 1 Kinematic diagram of a vehicle with n=2 driving wheels



generalized rolling radius r_{ai}^0 in the driven mode. This radius is computed using the rolling radii of the right and left wheels, $r_{a1}^{0'}$ and $r_{a2}^{0''}$, in the driven mode (at zero wheel torque) [4]. In a conventional mechanical driveline, the equivalent wheels are connected with the transfer case by reduction gearings with gear ratios given by u_i , i=1,2. The angular velocity of the input shaft of the transfer case, ω_0 , is determined by the rotational velocity of the engine and the gear ratio of the transmission.

The equation of vehicle movement can be written down as

$$\sum_{i=1}^{2} F_{xi} - \sum_{i=1}^{2} R_{xi} - F_d \pm F_a - D_a \pm W_a \sin \theta_g = 0$$
 (1)

Where R_{xi} is rolling resistance of a wheel, F_d the drawbar pull force, F_a is the acceleration force, D_a the air drag force, $W_a \sin \theta_g$ the longitudinal component of the vehicle weight on a slope with angle θ_g , and F_{xi} the individual wheels' circumferential forces. The total circumferential force of the vehicle, $F_{x\Sigma}$, comes from Eq. (1) as follows

$$F_{x\Sigma} = \sum_{i=1}^{4} F_{xi} = \sum_{i=1}^{4} R_{xi} + F_d \pm F_a + D_a \pm W_a \sin \theta_g$$
 (2)

If the resistance to movement represented by the right hand-side of Eq. (2) is known, this equation allows for computing the sum of the circumferential wheel forces, i.e., the total circumferential force of the vehicle. However, Eq. (2) does not yet allow for determining the circumferential forces, i.e., for computing forces F_{xi} , i = 1, 4. This is presented next by considering the kinematic discrepancy factor.

In deriving an equation for the kinematic discrepancy factor, the total resistance to motion of the vehicle, described by the right hand-side of Eq. (2), is considered close to zero, i.e., $F_{x\Sigma} \rightarrow 0$. If the wheels were not connected by the frame and could move separately from each other, the theoretical velocity of each wheel in this mode would be determined by the equation

$$V_{ti} = \omega_{0i} r_{ai}^{0} = \frac{\omega_{0}}{u_{i}} r_{ai}^{0}$$
 (3)

where, ω_{0i} is the angular velocity of the single equivalent wheel differential, i.e., the rotational velocity of the differential that is installed between the right and left wheels of an axle.

However, it is obvious that the centers of all the wheels, which are connected to the vehicle's frame, move with the same velocity, i.e., V_a (see <u>Fig. 1</u>). This linear velocity of the vehicle in the travel mode with $F_{x\Sigma} \rightarrow 0$ is termed as the theoretical linear velocity.

The velocities, V_{ti} and V_a may not necessarily be equal to each other. The difference between them is defined as a kinematic discrepancy that is estimated by the factor of the i-th axle [4]

$$m_{Hi} = \frac{V_{ti} - V_a}{V_{ci}}, i = 1, n$$
 (4)

As seen from Eq. (4), the kinematic discrepancy factor's structure is similar to the tire slippage, which compares the theoretical velocity of a wheel to its actual velocity. In this regard, the physical meaning of the kinematic discrepancy factor is the slippage of a tire that is caused by the difference in the velocities V_{ti} and V_a when the vehicle is moving with $F_{x\Sigma} \rightarrow 0$. Depending on the magnitudes of the velocities, this tire slippage can be either positive or negative, i.e., some of the wheels may slip and others may skid.

Velocity V_a is defined by the following expression [4]:

$$V_a = \omega_0 r_a^0 \tag{5}$$

where r_a^0 is termed as the generalized rolling radius of the vehicle in the driven mode, reduced to the input shaft of the transfer case. Hence, the physical meaning of Eq. (5) is that the theoretical velocity is the linear velocity of an equivalent single wheel that rotates with rotational velocity ω_0 and has a rolling radius in the driven mode given by r_a^0 .

Upon substitution of Eq. (3) and (5), Eq. (4) transforms to the form of:

$$m_{Hi} = 1 - r_a^0 \frac{u_i}{r_{ai}^0}, i = 1, n$$
 (6)

When the total resistance to movement is close to zero, the relationship between the circumferential wheel force F_x , and the slippage, which is equal to the kinematic discrepancy factor in this mode of travel, becomes a linear function [4]

$$F_{xi} = K_{ai} m_{Hi} = K_{ai} \left(1 - r_a^0 \frac{u_i}{r_{ai}^0} \right), i = 1, n$$
 (7)

where, K_{ai} is the longitudinal stiffness of an equivalent wheel that represents an axle (see <u>Fig. 1</u>) that is determined by the longitudinal stiffness factors of the left and right wheels of the axle.

Since $F_{x\Sigma} \rightarrow 0$, then the sum of the axle torques, T_{ai} , reduced to the input shaft of the transfer case is equal to zero:

$$\sum_{i=1}^{n} \frac{T_{ai}}{u_i} = \sum_{i=1}^{n} \frac{F_{xi} r_{ai}^0}{u_i} = 0$$
 (8)

Substituting Eq. (7) in Eq. (8) results in the equation that determines the generalized rolling radius of the vehicle in the driven mode:

$$r_a^0 = \left(\sum_{i=1}^n K_{ai} r_{ai}^0 / u_i\right) \left(\sum_{i=1}^n K_{ai}\right)^{-1}$$
 (9)

Using Eq. (9) and Eq. (6), the kinematic discrepancy of the i-th axle of the vehicle is finally written as follows:

$$m_{Hi} = 1 - \frac{u_i}{r_{ai}^0} \frac{\sum_{i=1}^{n} K_{ai} r_{ai}^0 / u_i}{\sum_{i=1}^{n} K_{ai}}, i = 1, n$$
 (10)

This kinematic discrepancy equation expanded to include all four wheels, is

$$m_{Hi}^{(")} = 1 - \frac{u_i^{(")}}{r_{wi}^{0'(")}} r_a^0 = 1 - \frac{u_i^{(")}}{r_{wi}^{0'(")}} \frac{\sum_{i=1}^n K_{xi}^{(")} r_{wi}^{0'(")} / u_i^{(")}}{\sum_{i=1}^n K_{xi}^{(")}}, i = 1, n \quad (11)$$

where superscripts and refer to the left and right wheels; (C') includes both. Eq. (11) therefore expands into a set of four equations for the kinematic discrepancies of four wheels: m'_{H1} , m'_{H1} , m'_{H2} , and m''_{H2} . Each wheel has its own separate value of $u_i^{(C')}$, $r_{wi}^{(C')}$, and $K_{xi}^{(C')}$. Eq. (11) explicitly shows that the kinematic discrepancy factors can be controlled by controlling the gear ratios from the transfer case to the wheels and, also, by using wheels of different size with different stiffness properties and rolling radii in the driven mode. Eq. (11) is further used to determine functional relations between tire slippages when the vehicle loaded with a motion resistance that is greater than zero on real terrain.

Generalized Tire Slippages of Axles and Generalized Slippage of Vehicle

When the vehicle is loaded with a real resistance to its movement, i.e., $F_{x\Sigma} > 0$, the vehicle's linear velocity decreases from V_a to V_x ; this velocity drop can be characterized by a slippage factor that is introduced as the generalized slippage of the vehicle [4]

$$s_{\delta a} = \frac{V_a - V_x}{V} \tag{12}$$

whence

$$V_{r} = V_{a} \left(1 - s_{\delta a} \right) \tag{13}$$

On the other end, the actual velocity of the vehicle can be expressed in terms of the theoretical velocities of the wheels and the generalized tire slippages of the axles, $s_{\delta ai}$.

$$V_x = V_{t1}(1 - s_{\delta a1}) = V_{t2}(1 - s_{\delta a2}) = \dots = V_{tn}(1 - s_{\delta an}) \quad (14)$$

or

$$V_x = V_{ti}(1 - s_{\delta ai}), i = 1, n$$
 (15)

Equating Eqs. (13) and (15) and utilizing Eq. (4) results in the following equation for the generalized tire slippages of the axles, $s_{\delta ai}$ [4]

$$s_{\delta ai} = m_{Hi} + (1 - m_{Hi}) s_{\delta a}, i = 1, n$$
 (16)

Equation (16) illustrates the influence of the kinematic discrepancy factors on the generalized tire slippages of axles. If there is no kinematic discrepancy, the generalized tire

slippages and the generalized slippage of the vehicle are the same. If the total resistance to motion is very low $(F_{x\Sigma} \to 0)$ and the velocities V_{ti} and V_a are not the same, the generalized tire slippage of an i-th axle is equal to the kinematic discrepancy factor of that axle. Thus, for a vehicle moving over a road with a negligible resistance without traction load, the wheels are subject to slippage, leading also to a vehicle velocity loss and to corresponding power losses and in the wheel locomotion system.

Equations (10) and (16) are the key equations for solving Eq. (2) and, thus, determining the circumferential forces of the axles.

Tire Slippages and Circumferential Forces of Axles

The circumferential force at a wheel can be modeled as a nonlinear function of the tire slippage. Equation (17) is a traction characteristic in which terms k and the peak friction coefficient μ_{px} are properties of the tire and terrain [4].

$$F_x = \mu_{px} R_z \left(1 - e^{-ks_{\delta}} \right) \tag{17}$$

Using Eqs. (16) and (17), Eq. (2) can be re-written in the following form

$$\sum_{i=1}^{n} \mu_{pxi} R_{zi} (1 - \exp(-k_i |(m_{Hi} + (1 - m_{Hi}) s_{\delta a})|))$$

$$\frac{m_{Hi} + (1 - m_{Hi})s_{\delta a}}{|m_{Hi} + (1 - m_{Hi})s_{\delta a}|} = F_{x\Sigma}$$
(18)

For given terrain properties, the normal wheel reactions, and the kinematic discrepancy factors, Eq. (18) can be solved for the generalized vehicle slippage, $s_{\delta a}$. The tire slippages, $s_{\delta i}$, can then be computed using Eq. (10) and (16). Finally, the circumferential wheel forces can be computed with the use of Eqs. (17). This method to determine the circumferential forces of the front and rear wheels was applied to a 4×4 tactical vehicle with a gross mass of 8663 kg. In these simulations, the gear ratios from the transfer case to the front wheels and from the transfer case to the rear wheels were assigned as shown in Table 1, in which u_{fd} stands for the gear ratio of the final drive. While one gear ratio is kept constant and equal to u_{fd} , the other gear ratio changes from $0.1u_{fd}$ to $2u_{fd}$.

According to the changes of the gear ratios, the kinematic discrepancy factors of the front and rear axles computed from Eq. (10) follow the curve shown in Fig. 2.

Computational results of the tire slippages and the circumferential forces of the front and rear axles are given in Figs. 3 and $\underline{4}$ for the 4×4 vehicle on Norfolk Sandy Loam

TABLE 1 Combinations of Gear Ratios

Case Number	u ₁	u ₂
Case I	Variable	U_{fd}
Case II	U_{fd}	Variable
Case III	Variable	Variable

© SAE International.

FIGURE 2 Kinematic Discrepancy Factors

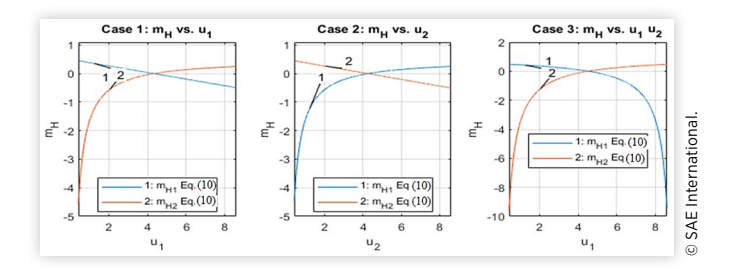


FIGURE 3 Tire Slippages of the Front and Rear Wheels

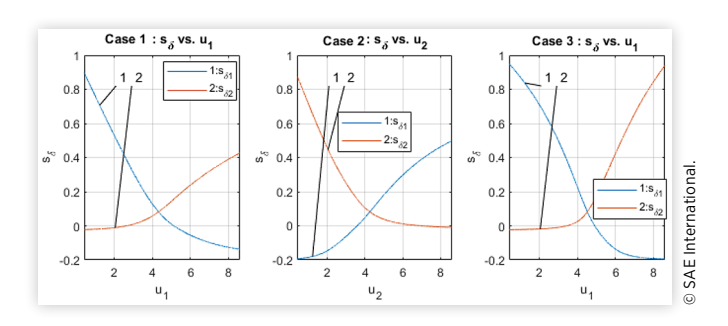
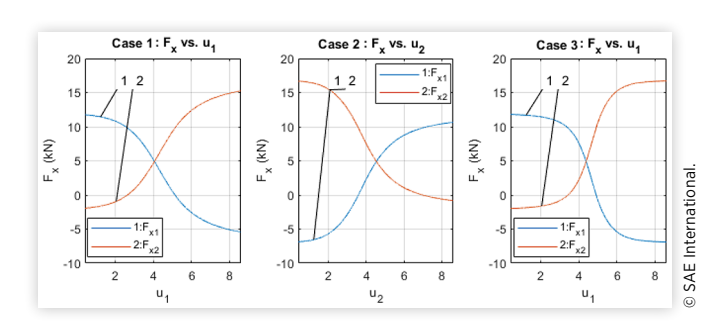


FIGURE 4 Circumferential Forces of the Front and Rear Wheels



soil [21]. As seen, due to the introduction of the kinematic discrepancy factors, the tire slippages and the circumferential forces vary within a wide range taking both positive and negative values.

New Method for Mobility Performance Assessment

To characterize the influence of the gear ratios and, thus, the power split between the front and rear wheels on vehicle mobility performance, a new *velocity-based mobility performance index* is proposed in the following form

$$\eta_{vmp} = \frac{V_x}{V_{a*}} \tag{19}$$

where, V_{a*} is the theoretical velocity of the vehicle when the gear ratios are the same and equal to the gear ratio of the final drive of the vehicle, u_{fd} . When the gear ratios are equal to u_{fd} ,

the generalized rolling radius of the vehicle in the driven mode from \underline{Eq} . (9) becomes

$$r_{a*}^{0} = \frac{K_{a1}r_{a1}^{0} + K_{a2}r_{a2}^{0}}{u_{fd}(K_{a1} + K_{a2})}$$
 (20)

and the vehicle theoretical velocity is defined as follows:

$$V_{a*} = \omega_0 r_{a*}^0 \tag{21}$$

The proposed index compares the actual velocity of a 4×4 vehicle, V_x , which can be achieved by changing gear ratios u_1 and u_2 , to the theoretical velocity of the base vehicle configuration that is designed with the same and constant gear ratios to the front and rear wheels. Thus, the index allows for assessing the influence of the power split between the wheels on vehicle actual velocity and, thus, on vehicle mobility performance.

<u>Figure 5</u> illustrates the velocity-based mobility performance index computed for case I, II, and III.

As seen from Fig. 5, the velocity-based mobility performance index is lower than unity in case III, but it can be greater that unity in case I and II. To explain such behavior of the curves in Fig. 5, the *generalized slippage factor to assess velocity losses* is introduced here

$$s_{\delta v} = \frac{V_{a*} - V_x}{V_{a*}} = 1 - \eta_{vmp}$$
 (22)

<u>Figure 6</u> graphically reflects the generalized slippage factor in the three cases.

Negative magnitudes of $s_{\delta\nu}$ indicates the skid effect, not the slip effect. This fact prompts a comparison of the data in Fig. 6 to Figs. 3 and 4. As seen, the generalized slippage factor to assess velocity losses becomes negative when tire slippage of the front wheels (case I) and tire slippage of the rear wheels

FIGURE 5 Velocity-based mobility performance index

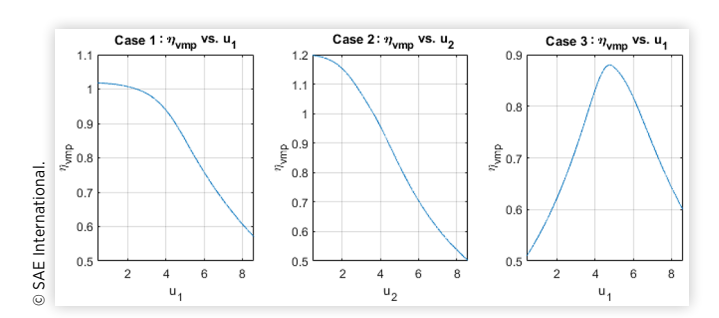


FIGURE 6 Generalized Slippage Factor to Assess Velocity Losses

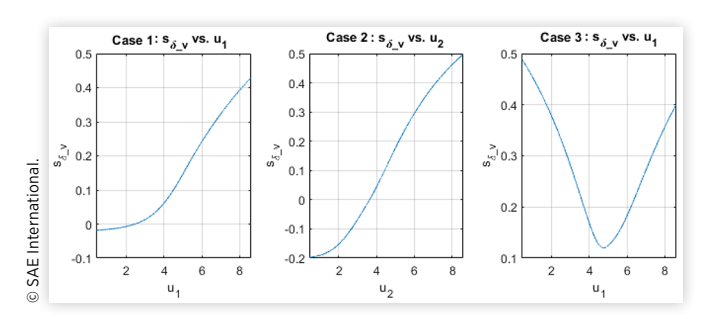


TABLE 2 Mobility Performance Characteristics (Case III)

η_{vmp}^{max}	$\mathcal{S}^{min}_{\delta V}$	U _i mo	U ₂ ^{mo}	S _{δl} ^{mo}	S ^{mo} δ2
0.880	0.120	4.774	4.256	0.027	0.126
				© SAE II	nternational.

(case II) are negative. In both cases, the circumferential force at the wheels of one axle (either the front or rear axle) is negative. Thus, either the front or rear wheels are in skid.

Having a negative circumferential force at one of the two drive axles increases the resistance to vehicle movement, and, thus, the other drive axle must develop a bigger positive circumferential force to overcome both the vehicle rolling resistance and the negative circumferential force. As seen from Figs. 2 through $\underline{6}$, due to a change of one or two gear ratios u_1 and u_2 , the kinematic discrepancy factors vary in a wide range that leads to different tire slippages and circumferential forces at the front and rear wheels.

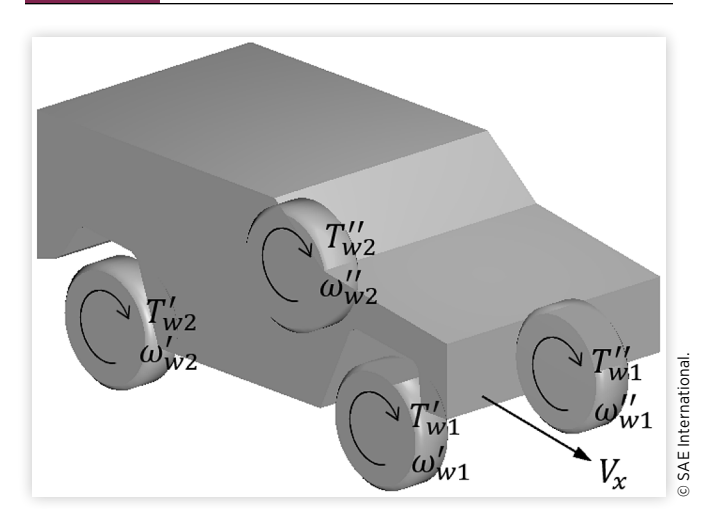
Reasonable boundaries for varying the gear ratios are constrained by zero values of the circumferential forces (zero tire slippages). These boundaries for the range in u_1 and u_2 can be seen in Figs. 3 and 4 where the circumferential force and tire slippage reach negative values. In case I (see Fig. 5), the varying of gear ratio u_1 from 5.14 to the value of 2.65 while $u_2 = u_{fd} = 4.3$ can provide a 19% increase in the velocity-based Mobility Performance Index. The increase of η_{vmp} reaches 42% in case II when gear ratio u_2 is decreased from 6.98 to 3.60 within the established boundaries while gear ratio u_1 is kept constant, $u_1 = u_{fd} = 4.3$. In case III, values of the two gear ratios can be established to provide the maximum of the velocitybased mobility performance index. As seen from Fig. 5, the maximum value of $\eta_{vmp}^{max} = 0.880$ is provided when the values of the gear ratios are $u_1^{mo} = 4.774$ and $u_2^{mo} = 4.256$, which correspond to the minimum of the generalized slippage factor, which assesses the velocity losses, $s_{\delta v}^{min} = 0.120$, shown in Fig. 6. These u_1^{mo} and u_2^{mo} provide the maximum of vehicle mobility performance for the range of u_1 and u_2 in case III.

One more important observation follows from the above analysis. The velocity-based mobility performance index reaches its maximum in case III at non-equal slippages of the front and rear tires as illustrated in <u>Table 2</u>. Tire slippages $s_{\delta 1}^{mo}$ and $s_{\delta 2}^{mo}$ can be named as the slippages that provide the maximum of mobility performance of the vehicle.

Mathematical Model of Virtual Driveline System That Provides Optimal Power Distributions to Maximize Mobility of the Vehicle

<u>Figure 7</u> depicts a 4×4 vehicle in which the mechanical driveline is replaced with four individual e-motors providing torque to each wheel. The four wheel torques $T_{wi}^{('')}$ and angular velocities $\omega_{wi}^{('')}$ may be set individually. The generalized vehicle

FIGURE 7 4×4 vehicle with wheels driven by 4 e-motors



parameters provide the basis for the Virtual Driveline System (VDS) that defines the relationships between individual wheel dynamics and overall vehicle dynamics.

The basis for these relationships is the wheels' kinematic discrepancy factors (see Eq. (4)). As shown in Eq. (11), kinematic discrepancy is a function of the generalized rolling radii in the driven mode, the tire longitudinal stiffness, and the gear ratios between the wheels and transfer case.

In the VDS with four e-motors, the two physical gear ratios u_i do not exist and become four virtual signals, $u_i^{('')}$. These inputs $u_i^{('')}$ are defined as the change in wheel's angular velocity $\omega_{wi}^{('')}$ from the baseline value of ω_0 , the value it would take if $u_i^{('')} = 1$ [4]:

$$\omega_{wi}^{'(")} = \frac{\omega_0}{u^{(")}} \tag{23}$$

 r_a^0 can be calculated using Eq. (24), by expanding Eq. (9) to four wheels [4]:

$$r_a^0 = \left(\sum_{i=1}^n K_{xi}^{'(i')} r_{wi}^{0'(i')} / u_i^{'(i')}\right) \left(\sum_{i=1}^n K_{xi}^{'(i')}\right)^{-1}$$
(24)

When the vehicle is loaded with a real resistance to its movement, i.e., $F_{x\Sigma} > 0$, the vehicle linear velocity decreases from V_a to V_x ; this velocity drop can be characterized by a slippage factor that is introduced as the generalized slippage of the vehicle [4] (Eqs. (12-13)). From Eq. (16), the individual tire slippages $s_{\delta i}^{('')}$ are related to the generalized vehicle slippage $s_{\delta a}$ through their kinematic discrepancy factors. With zero kinematic discrepancy, tire slippage $s_{\delta i}^{('')}$ would be equal to the generalized vehicle slippage $s_{\delta a}$. Changing $m_{Hi}^{(''')}$ allows changing the slippages, $s_{\delta i}^{(''')}$. To calculate the effect this has on the power distribution, the exponential traction equation (Eq. (17)) is used as the starting point:

$$F_{xi}^{('')} = \operatorname{sign}\left(s_{\delta i}^{('')}\right) \mu_{pxi}^{('')} R_{zi}^{('')} \left(1 - e^{-k_i^{('')} \left|s_{\delta i}^{('')}\right|}\right)$$
 (25)

The absolute value and sign functions are used to account for a negative slippage (skid). All four wheels' circumferential forces add up to the total circumferential force $F_{x\Sigma}$. The total circumferential force is calculated with Eq. (2). Summing all four $F_{xi}^{(")}$, equating the result to $F_{x\Sigma}$, and replacing $s_{\delta i}^{(")}$ in Eq. (25) with the right side of Eq. (16) results in Eq. (26).

$$\sum_{i=1}^{2} sign\left(m_{Hi}^{(i')} + \left(1 - m_{Hi}^{(i')}\right) s_{\delta a}\right) \mu_{pxi}^{(i')} R_{zi}^{(i')}$$

$$\left(1 - e^{-k_{i}^{(i')} \left|m_{Hi}^{(i')} + \left(1 - m_{Hi}^{(i')}\right) s_{\delta a}\right|}\right) = F_{x\Sigma}$$
(26)

Equations (23) through (26) taken together with Eq. (11) make up the model of the Virtual Driveline System. The idea behind the VDS is that while the four wheels' drives are independently controlled, their dynamics are linked. The kinematic discrepancies of the four wheels are interdependent as shown by the four factors $u_i^{('')}$ Eq. (11). These four values of $u_i^{('')}$ represent "virtual gear ratios" that may be controlled to influence the kinematic discrepancies. These kinematic discrepancies in turn affect the rolling radii and slippages, generalized to the vehicle, in Eqs. (24) and (26).

Mobility Optimization of Virtual Driveline System

The mathematical equations of the VDS create a model of a driveline with a controllable torque split using four individual ratios, $u_i^{(n)}$. To optimize mobility, optimal values of $u_i^{(n)}$ must be found which correspond to the maximum of the mobility index for any moment of time.

For the objective function, velocity-based mobility performance index η_{vmp} (Eq. (19)) is used. Equation (19) must be put in terms of $u_i^{(r')}$ to calculate η_{vmp} for any distribution of $u_i^{(r')}$. In Eq. (21), V_{a*} is equal to ω_0 multiplied by r_{a*}^0 . Radius r_{a*}^0 is the generalized rolling radius of the vehicle in the driven mode when the gear ratios are equal to a final drive value u_{fd} in a conventional driveline with fixed ratios. For the VDS with four wheels and four controllable inputs $u_i^{(r')}$, r_a^0 is given by Eq. (24). Setting $u_i^{(r')} = u_{fd}$ in Eq. (24) gives Eq. (27) for r_{a*}^0 :

$$r_{a*}^{0} = \frac{\sum_{i=1}^{4} K_{xi}^{(\prime\prime)} r_{wi}^{0\prime(\prime\prime)}}{u_{fd} \left(\sum_{i=1}^{4} K_{xi}^{(\prime\prime)}\right)}$$
(27)

Using Eqs. (5), (12), and (20), V_{a*} can be expressed as

$$V_{a*} = \frac{V_x}{r_a^0 (1 - s_{\delta a})} r_{a*}^0 \tag{28}$$

Plugging Eq. (28) into Eq. (19) gives

$$\eta_{vmp} = \left(1 - s_{\delta a}\right) \frac{r_a^0}{r_{a*}^0} \tag{29}$$

Eq. (29) illustrates that η_{vmp} will depend on both the values of the generalized vehicle slippage and the generalized

rolling radius in the driven mode. Substituting r_a^0 from Eq. (24) and r_{a*}^0 from Eq. (27) into Eq. (29) transforms η_{vmp} to

$$\eta_{vmp} = \left(1 - s_{\delta a}\right) u_{fd} \frac{\sum_{i=1}^{n} K_{xi}^{'(i')} r_{wi}^{0'(i')} / u_{i}^{'(i')}}{\sum_{i=1}^{n} K_{xi}^{'(i')} r_{wi}^{0'(i')}}$$
(30)

Equation (30) gives a method to calculate η_{vmp} from the generalized slippage $s_{\delta a}$ and gear ratios $u_i^{('')}$. The method to optimize Eq. (30) is given in the project report [21].

After determining optimal $u_i^{('')}$ from Eq. (30), r_a^0 can be computed from Eq. (24). Using r_a^0 and $s_{\delta a}$ from Eq. (26), η_{vmp} can be calculated from Eq. (29). Using Eq. (19), η_{vmp} will give a value of the actual velocity V_x different from the theoretical velocity V_{a*} , which is the velocity the vehicle would take without slippage and without controllable gear ratios. This value of V_x can be considered the potential improved velocity over the theoretical velocity V_a under optimization of the kinematic discrepancy factors. Therefore, η_{vmp} quantifies vehicle mobility as improvements in its velocity resulting from controlling the gear ratios to alter the slippage and kinematic discrepancy.

Computational Results

Two vehicle drivelines were modeled to compare mobility performance using computer simulations of the 4x4 vehicle on terrain:

- 1. "Conventional Driveline", i.e., Open Differential Driveline System: A conventional driveline with three open differentials (one differential in the transfer case and two differentials in the drive axles)
- "Virtual Driveline System", i.e., VDS: A system in which the e-motors are managed via a virtual driveline with the optimal characteristics to provide the maximum mobility of the 4x4 vehicle in given terrain conditions

The Open Differential Driveline System (number 1) splits power to the wheels via three open differentials, in which each of them has a differential gear ratio of unity. The vehicle motion was simulated on deformable soil, which was accepted as Norfolk Sandy Loam [22]. All plotted data is presented for 1 sec of motion, but statistic characteristics (given in tables) were determined moving through 1000 meters of generated stochastic terrain.

Computational Tire-Terrain Characteristics

<u>Figure 8</u> illustrates stochastic changes of the peak friction coefficient, μ_{px} , under the four wheels of the vehicle moving on soil terrain. The method presented before in reference [23] was used for this simulation: terrain values are modeled as continuously changing stochastic variables. These stochastic

FIGURE 8 Peak friction coefficient on soil of the front and rear tires

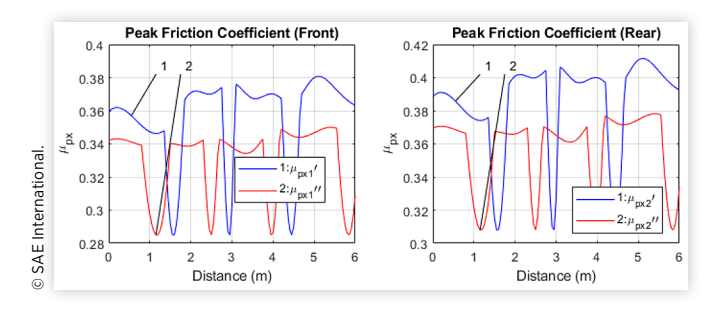
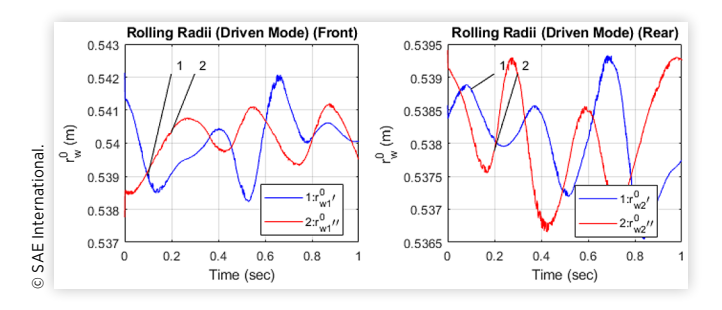


FIGURE 9 Rolling radius in the driven mode of the front and rear tires



values are fed into Eq. (25) to simulate the exponential relationship between the circumferential wheel force and tire slippage.

The stochastic changes of the terrain also impact the tire rolling radius in the driven mode (i.e., at zero torque) and is illustrated in Fig. 9.

All above-presented tire-terrain settings were utilized to simulate the movement of the vehicle with the two different drivelines.

The following sections discuss the traction force distribution, tire slippages, and other characteristics and metrics of mobility of the vehicle with two drivelines.

Circumferential Wheel Forces, Tire Slippages, Vehicle Generalized Slippage

<u>Figure 10</u> presents the circumferential wheel forces, tire slippages and the generalized slippage of the vehicle with the conventional driveline moving on the soil terrain.

The traction-slippage characteristics of the vehicle with the optimized driveline are given in Fig. 11. The circumferential wheel forces in Fig. 11 should be considered the optimal forces for mobility, i.e., their numerical values correspond to the maximum vehicle mobility in the given stochastic terrain conditions. These forces are developed at the driving wheels by changing the gear ratios between the e-motors and the driving wheels to provide the maximum velocity-based mobility performance index (see Eq. (19). The physics here is that a change of the gear ratios leads to a change in the kinematic discrepancy factors (Eq. (11)) and the generalized rolling radius of the vehicle in the driven mode (Eq. (24)). Both tire

FIGURE 10 Circumferential wheel forces, tire slippages and the generalized slippage of the vehicle with the conventional driveline on soil terrain

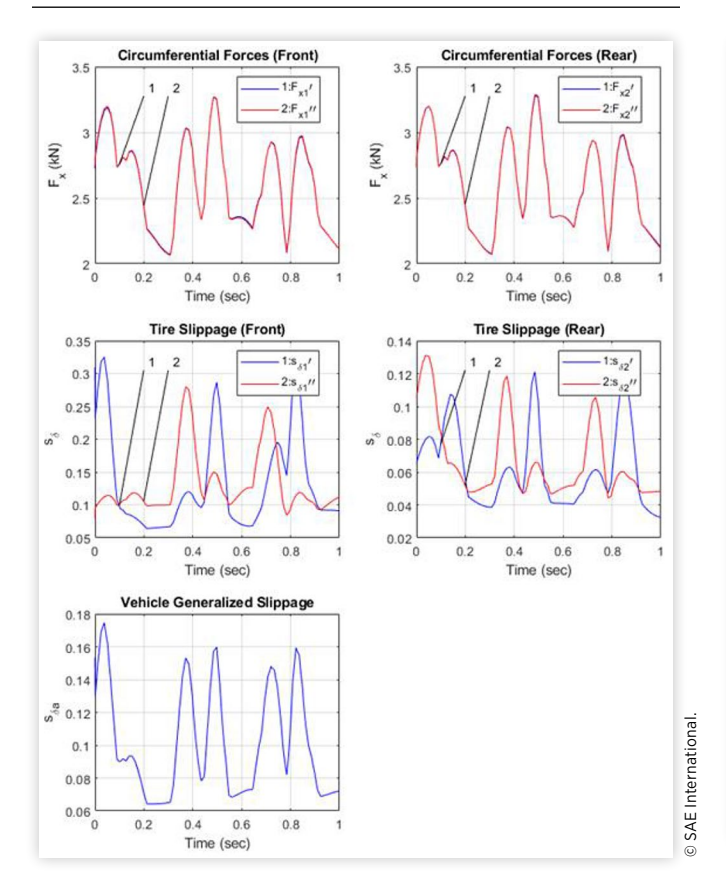
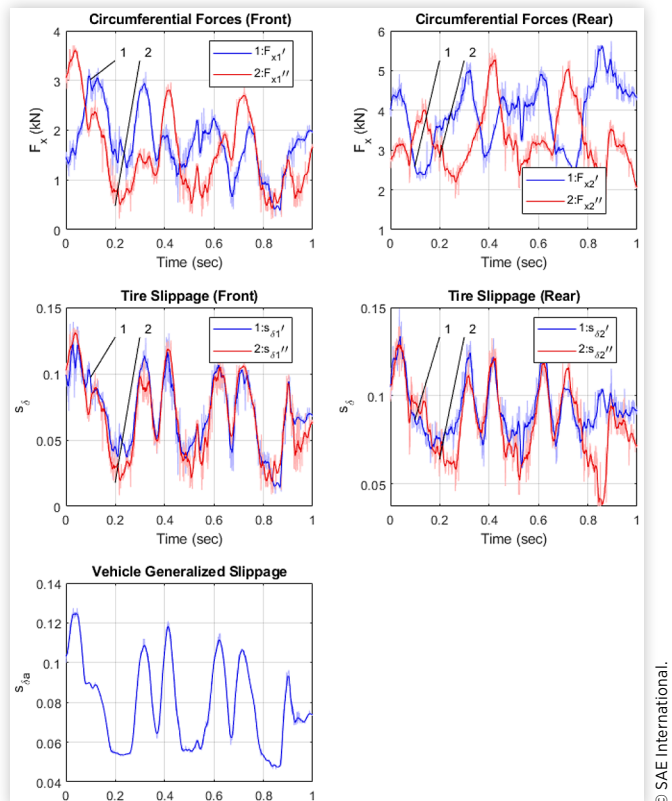


FIGURE 11 Circumferential wheel forces, tire slippages and the generalized slippage of the vehicle with the optimized driveline on soil terrain



slippages and the vehicle generalized slippage change according to the changes of the kinematic discrepancy factors (see Eq. (16)); the latter impact the circumferential wheel forces, which come from Eq. (25).

As seen in Fig. 11, the circumferential forces of the left and right wheels can take different values. The maximum difference was 3.9 kN. Equation (31) is used to calculate the effect of this traction difference on the vehicle's lateral dynamics:

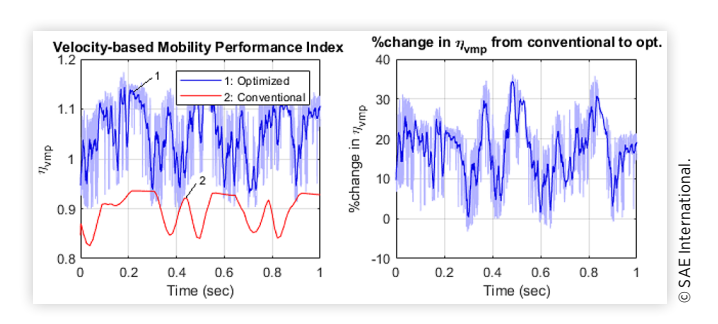
$$\alpha^{max} = \frac{\left(0.5B_t\right)\Delta F_{xLR}^{max}}{4C_{\alpha}l_2} \tag{31}$$

where B_t is the tread (the distance between the left and right wheels), ΔF_{xLR}^{max} is the maximum difference between left and right circumferential forces, C_α is the tire cornering stiffness, and l_2 is the wheelbase. α^{max} is the maximum side slip angle at any single wheel caused by the difference in left/right forces. α^{max} was 0.08 deg; the impact on the yaw is negligible and would not be more than a locked differential would generate in a conventional vehicle with locking differential.

Mobility Performance Assessment

As the main result of the optimization of the gear ratios, Fig. 12 graphically presents the velocity-based mobility

FIGURE 12 Velocity-based mobility performance index of the vehicle with two drivelines (left), comparison of the conventional driveline to the optimized driveline (right)



performance index of the vehicle with the two drivelines on soil terrain.

As seen from Fig. 12, the optimization of the gear ratios results in a significant improvement of the mobility performance on soft deformable soil. The velocity-based mobility performance index of the vehicle with the optimized driveline is greater than unity. This means that the actual velocity of the vehicle with the optimized driveline, which is computed based on tire slippages, is greater than the theoretical velocity (i.e., the velocity at zero slippage) of the same vehicle with a basic driveline (see more on the velocity-based mobility performance index at Eq. (19)).

TABLE 3 Velocity-based mobility performance index

al.	Driveline	Optimized. vs.		
ation	Optimized	Conventional	Conventional	
E Internationa	renormance maex		Percentage Increase	
© SA	1.0462	0.8972	16.61%	

FIGURE 13 Actual velocity of the vehicle with two drivelines (left), comparison of the conventional driveline to the optimized driveline (right)

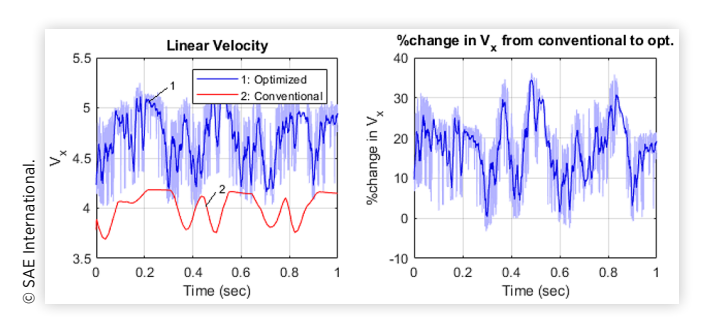


TABLE 4 Mean Actual Velocity

Driveline		Optimized. vs.	
Optimized	Conventional	Conventional	
Mean Actual Velocity, m/sec		Percentage Increase	
4.6771	4.0109	16.61%	

© SAE International.

Complementary to Fig. 12 information, Table 3 presents the mean values of the velocity-based mobility performance index and comparison of the mean values on different terrains and with different drivelines. The maximization of mobility by optimizing the gear ratios to the driving wheels resulted in a significant increase of the velocity-based mobility performance index on soft soil.

In addition to the velocity-based mobility performance index, <u>Fig. 13</u> provides actual velocities of the vehicle with two different drivelines on soft soil.

<u>Table 4</u> supplements <u>Fig. 13</u> by providing the mean values of the actual velocity of the vehicle with different drivelines on different terrains.

Summary/Conclusions

To assess mobility performance, a new velocity-based mobility performance index was introduced. The velocity-based mobility performance index compares the actual velocity of a vehicle having any advanced power split between the driving wheels to the theoretical velocity of the base vehicle configuration, i.e., the configuration with a mechanical driveline system that is designed with the same and constant gear ratios from the transfer case to the front and rear wheels.

A detailed analysis of the proposed velocity-based mobility performance index and its' components was

conducted and practical directions to increase mobility were introduced by selecting appropriate vehicle generalized parameters. The velocity-based mobility performance index is further used as an objective function to maximize the mobility performance by optimizing the power split between the driving wheels.

The velocity-based mobility performance index was used as the objective function for the wheel power distribution optimization that was conducted by introducing the gear ratios of the gear sets, which connect the e-motors to the wheels, as the optimization parameters. The optimization allows for increasing the mobility performance up to 16.6 % on soft soil (Norfolk Sandy Loam in this study).

The proposed velocity-based mobility performance index was proven as a suitable index to assess mobility performance by comparing the actual velocity of a vehicle to the theoretical velocity of the same vehicle with a basic configuration of the driveline system.

The conducted study on the optimization of the mobility performance creates a possibility to design control algorithms for real-time controlling and maximizing vehicle mobility performance. This study is a part of a control strategy development that includes a control of vehicle stability.

References

- 1. Gray, J., Vantsevich, V., and Paldan, J., "Agile Tire Slippage Dynamics for Radical Enhancement of Vehicle Mobility," *Journal of Terramechanics* 65:14-37, 2016.
- Larin, V., "Theory of Motion of all-Wheel Drive Vehicles," Bauman, N. MSTU Press, Moscow, 2010.
- 3. Smirnov, G., *Theory of Motion of Wheeled Vehicles* 2nd Edition (Moscow: Mashinostroenie, 1990).
- Andreev, A., Kabanau, V. and Vantsevich, V., "Driveline of Ground Vehicles: Theory and Design," Vantsevich, V.V., Scientific and Engineering Editor; Taylor & Francis Group/ CRC Press, 792, 2010.
- 5. Ageikin, Ya., "*Mobility of Automobiles*,", (Moscow: Mashinostroenine Publisher, 1981) (in Russian).
- 6. Lee, C., Hedrick, K., and Yi, K., "Real-Time Slip-Based Estimation of Maximum Tire-Road Friction Coefficient," *IEEE/ASME Transactions on Mechatronics* 9(2):454-458, 2004, doi:10.1109/TMECH.2004.828622.
- Wong, J., "An Introduction to Terramechanics," *Journal of Terramechanics* 21(1):5-17, 1984, https://doi.org/10.1016/0022-4898(84)90004-1.
- Wismer, R., and Luth, H., "Off-Road Traction Prediction for Wheeled Vehicles," *Journal of Terramechanics*, 10, 2,1973, 49-61,0022-4898, https://doi.org/10.1016/0022-4898(73)90014-1.
- Wismer, R., "Soil Dynamics: A Review of Theory and Application," SAE Technical Paper 820656, 1982, https://doi.org/10.4271/820656.
- Gee-Clough, D., McAllister, M., Pearson, G., and Evernden, D., "The Empirical Prediction of Tractor-Implement Field Performance," *Journal of Terramechanics* 15(2):81-94, 1978, https://doi.org/10.1016/0022-4898(78)90026-5.

- 11. Janosi, Z. and Hanamoto, B., "The Analytical Determination of Drawbar Pull as a Function of Slip for Tracked Vehicles in Deformable Soils," in *First ISTVS International Conference*, Turin, 1961, 707-736.
- 12. Wang, G. and Zoerb, G., "Indirect Determination of Tractor Tractive Efficiency," *Canadian Agricultural Engineering* 32(2):243-248, 1990. https://www.cabdirect.org/cabdirect/abstract/19912447592.
- 13. Li, Y., Zhang, J., Guo, K., and Wu, D., "Optimized Torque Distribution Algorithm to Improve the Energy Efficiency of 4WD Electric Vehicle," SAE Technical Paper 2014-01-2374, 2014, https://doi.org/10.4271/2014-01-2374.
- Zhenpo, W., Changhui, Q., Xue, X., and Lei, Z., "Design and Control Strategy Optimization for Four-Wheel Independently Actuated Electric Vehicles," *Energy Procedia* 105:2323-2328, 2017, https://doi.org/10.1016/j.egypro.2017.03.667.
- Gao, L., Xiong, L., Gao, X., and Yu, Z., "Optimal Torque Allocation for Distributed Drive Electric Skid-Steered Vehicles Based on Energy Efficiency," SAE Technical Paper 2018-01-0579, 2018, https://doi.org/10.4271/2018-01-0579.
- Li, Y., Zhang, J., Guo, K., and Wu, D., "A Study on Force Distribution Control for the Electric Vehicle with Four In-Wheel Motors," SAE Technical Paper <u>2014-01-2379</u>, 2014, https://doi.org/10.4271/2014-01-2379.
- Kang, J., Kyongsu, Y., and Heo, H., "Control Allocation Based Optimal Torque Vectoring for 4WD Electric Vehicle," SAE Technical Paper <u>2012-01-0246</u>, 2012, <u>https://doi.org/10.4271/2012-01-0246</u>.
- Yamakawa, J., Kojima, A., and Watanabe, K., "A Method of Torque Control for Independent Wheel Drive Vehicles on Rough Terrain," *Journal of Terramechanics* 44(5):371-381, 2007, https://doi.org/10.1016/j.jterra.2007.10.006.
- Salama, M., Vantsevich, V., Way, T., and Gorsich, D., "UGV with a Distributed Electric Driveline: Controlling for

- Maximum Slip Energy Efficiency on Stochastic Terrain," *Journal of Terramechanics* 79:41-57, 2018, https://doi.org/10.1016/j.jterra.2018.06.001.
- Vantsevich, V., Paldan, J., and Gray, J. "A Hybrid-Electric Power Transmitting Unit for 4x4 Vehicle Applications: Modeling and Simulation," 2014, V003T44A002, <u>10.1115/</u> DSCC2014-5855.
- Vantsevich, V., et al., "Optimization of Wheel Power Distribution to Maximize Multi-Wheel Drive Vehicle Mobility, Project Report for U.S. Army CCDC GVSC," 2019.
- 22. Salama, M., Way, T., and Vantsevich, V., "Parameterization of Norfolk Sandy Loam Properties for Stochastic Modeling of Light in-Wheel Motor UGV," in *Proceedings of the 8th Americas Regional Conference of the International Society of Terrain Vehicle Systems*, Troy, MI, 2016.
- Gray, J., Vantsevich, V., Opeiko, A., and Hudas, G., "A Method for Unmanned Ground Wheeled Vehicle Mobility Estimation in Stochastic Terrain Conditions", in *Proc. of the* 7th Americas Regional Conference of the ISTVS, Tampa, FL. 2013.

Contact Information

Jesse Paldan

University of Alabama at Birmingham Birmingham, AL jpaldan@uab.edu

Acknowledgments

This research was funded by the US Army CCDC Ground Vehicle Systems Center and partially by the National Science Foundation (award IIS-1849264)

^{© 2020} SAE International. All rights reserved. No part of this publication may be reproduced, stored in a retrieval system, or transmitted, in any form or by any means, electronic, mechanical, photocopying, recording, or otherwise, without the prior written permission of SAE International.